Theoretical and Experimental Studies on the Gas Transport Properties of Mixed Matrix Membranes Based on Polyvinylidene Fluoride

ARTICLE *in* AICHE JOURNAL · DECEMBER 2013

Impact Factor: 2.75 · DOI: 10.1002/aic.14186

2 AUTHORS, INCLUDING:

Yi Shen
South China University of Technology
27 PUBLICATIONS **313** CITATIONS

Theoretical and Experimental Studies on the Gas Transport Properties of Mixed Matrix Membranes Based on Polyvinylidene Fluoride

Yi Shen and Aik Chong Lua
School of Mechanical and Aerospace Engineering, Nanyang Technological University, 50 Nanyang Avenue, Singapore 639798, Republic of Singapore

DOI 10.1002/aic.14186
Published online August 1, 2013 in Wiley Online Library (wileyonlinelibrary.com)

The effects of the impregnation of three types of inorganic fillers into polyvinylidene fluoride (PVDF) polymer membranes on the gas permeability and selectivity of these membranes were studied theoretically and experimentally. Permeabilities of He, CO_2, O_2, and N_2 through three types of mixed matrix membranes (MMMs) based on PVDF, that is, PVDF/SiO_2, PVDF/MCM-41, and PVDF/4A MMMs, were experimentally measured and theoretically predicted using Maxwell, Higuchi, Bruggeman, and Bottcher-Landauer models. Theoretical permeabilities of the PVDF/SiO_2 MMMs using the above four models predicted the results in the following order: Maxwell model>Bruggeman model>Bottcher model>Higuchi model. However, this sequence was reversed for PVDF/MCM-41 MMMs. The nonporous SiO_2, mesoporous MCM-41 and zeolite 4A inorganic fillers had effects on the permeabilities of the challenge gases for the PVDF/SiO_2, PVDF/MCM-41, and PVDF/4A MMMs but had no effects on the selectivities of the MMMs. The experimental permeabilities of the MMMs showed that there were no significant differences among the three types of MMMs despite that the inorganic fillers, that is, SiO_2, MCM-41, and zeolite 4A, had distinct dissimilar properties such as pore structures and particle sizes. Density measurements indicated that some voids were present in the polymer/particle interfaces. Based on the density measurement results, the void volume fractions of the resulting MMMs were calculated. An equation is derived to determine the void thickness of the MMM in terms of its physical properties and hence this proposed equation can substitute the difficult task of measuring such void thickness through any microscopy techniques. The Maxwell, Higuchi, Bruggeman, and Bottcher-Landauer models could not predict the actual gas permeabilities of the PVDF MMMs. By taking the effects of crystallinity and immobilization factor on gas permeability into consideration, the extended modified Maxwell model showed good agreement with the experimental gas permeabilities of the resulting MMMs, indicating that the model did capture the essence of the gas transport behaviors through the MMMs. © 2013 American Institute of Chemical Engineers *AIChE J*, 59: 4715–4726, 2013

Keywords: MMM, permeability modeling, crystallinity and PVDF

Introduction

Mixed matrix membranes (MMMs) have been of great interest for gas separation.[1–5] With the combination of the desirable properties of polymer matrix and inorganic fillers, MMMs are expected to exhibit better performance to break the well-known trade-off relationship[6,7] between permeability and selectivity of polymer membranes for gas separation. The gas transport properties of MMMs with ideal organic–inorganic interface properties can be theoretically predicted by some models such as Maxwell, Higuchi, Bruggeman, and Bottcher-Landauer models.[3,8,9] These models treat MMMs to be ideal two phases. However, it was found that the gas transport properties of MMMs were highly dependent on the organic–inorganic interface properties. Moore and Koros[10] observed some nonideal factors of the interface including polymer chain rigidifications, void formation, and inorganic pore blockages that would affect the modeling work and they modified the Maxwell equation according to the properties of the interface.

The effects of polymer crystallinity on the gas transport properties were widely investigated.[11–13] Generally, crystallinity tends to reduce diffusion coefficient as well as solubility coefficient, thereby resulting in lower permeability of polymer membranes. Polyvinylidene fluoride (PVDF) is a well-known semicrystalline polymer and widely used as a membrane material in industry.[14–16] In this study, gas (He, CO_2, O_2, and N_2) permeabilities of three types of MMMs, that is, PVDF/SiO_2, PVDF/MCM-41, and PVDF/4A MMMs, were experimentally determined and also theoretically predicted using Maxwell, Higuchi, Bruggeman, Bottcher-Landauer, and modified Maxwell models. It is desirable to determine a suitable model that will provide a good correlation between the experimental and modeling results for gas

Correspondence concerning this article should be addressed to A.C. Lua at maclua@ntu.edu.sg.

permeabilities. The effects of crystallinity and the immobilization factor on the gas transport properties of the MMMs are to be considered.

Experimental

Materials

PVDF (Mw = 534,000) and its solvent, N-methyl-2-pyrrolidinone (NMP), nonporous nano-silica powder (particle size = 7 nm and Brunauer-Emmett-Teller (BET) area = 390 m^2/g) and zeolite 4A powder (particle size = 2.5 μm, pore size = 0.38 nm, and BET = 560 m^2/g) were purchased from Sigma Aldrich (Singapore). The nano-silica and zeolite 4A powders were activated at 180°C overnight under vacuum before use. The mesoporous MCM-41 (particle size = 56 nm, pore size = 2.7 nm, and BET = 817 m^2/g) was synthesized according to the method reported by Grun et al.[17] All these chemicals were used as received.

The procedures for the preparation of each type of PVDF MMM are as follows. A predetermined amount of each inorganic filler, that is, silica powder, zeolite 4A powder or MCM-41, was added to the NMP solvent and the mixture was ultrasonicated for 30 min. At first, 2% of the total amount of PVDF was then added into the NMP/filler mixture solution. After the initial loaded polymer was totally dissolved by stirring for 12 h and followed by a period of 30 min ultrasonication, the remaining PVDF polymer was added to the PVDF/NMP/filler solution and the final mixture was stirred for at least two days at room temperature (25 ± 1°C). Before casting, the final mixture was sonicated for 30 min to remove any gas bubbles and then it was cast on a clean silicon wafer. The resulting cast membranes were transferred into a vacuum oven and the temperature was raised to 120°C and dwelled for 24 h to remove the residue solvent.

A differential scanning calorimeter (DSC Q200 TA Instruments) was used to determine the phase transitions of the polymer membranes. The DSC tests were conducted at a temperature range of 40–200°C. First, the samples were equilibrated at 40°C and then heated to 200°C using a heating rate of 10°C/min. After being held isothermally at 200°C for 5 min to completely melt PVDF polymer, the samples were cooled from 200 to 40°C at a rate of 10°C/min. The tests were run for two cycles. The crystallinity (χ) of the samples was calculated using the following equation

$$\chi = \frac{\Delta H}{W \times \Delta H^0} \times 100\%$$

where ΔH is the fusion heat of the membrane, W is the PVDF weight content in the composite membranes, and ΔH^0 is the fusion heat of PVDF with 100% crystallinity of α phase, which was set to be 90.4 J/mol.[18]

The density of the sample was measured using an ultrapycnometer (Quantachrome Instruments). Helium was used as the probe gas and the working cell size was medium. For each test, the number of runs was set at 20 and the average value of the last four tests was presented on condition that the deviation was less than 0.1%.

Single gas permeation tests on the membranes were conducted using a constant volume, varying pressure experimental set-up as described in Lua and Su.[19] The single gases used in these tests were He, N_2, O_2, and CO_2. Each gas was of a purity of 99.99%. All the tests were carried out at room temperature and the feed pressure was set at 4 bars. The effective area of the membrane in the permeation test set-up was 4.9 cm^2. The gas permeability P was determined in accordance to that given by Shen and Lua[20] and its unit is in Barrer [1 Barrer = 1×10^{-10} cm^3 (Standard Temperature and Pressure) cm/(cm^2 s cm Hg)]. The permeabilities of He, CO_2 and O_2 were highly reproducible. However, as N_2 permeation was very slow, three tests for each sample were carried out and the average permeability value was used. The thickness of the membrane was measured by a micrometer. For each membrane, three measurements on different locations were conducted and the average value was obtained.

Modeling work

Maxwell model

Mathematically, several theoretical models have been proposed to predict the gas transport properties of MMMs. Maxwell first developed a model to analyze the steady-state permittivity of a dilute suspension of spheres. Subsequently, this model was analogously used to predict the gas permeability of MMMs. The model is as follows[21]

$$P_{\text{eff}} = P_c \left[\frac{nP_d + (1-n)P_c - (1-n)\phi_d(P_c - P_d)}{nP_d + (1-n)P_c + n\phi_d(P_c - P_d)} \right] \quad (1)$$

where P_{eff}, P_c, and P_d are the permeabilities of the MMMs, continuous phase, and dispersed phase, respectively, $\phi_d$is the volume fraction of the inorganic filler and n is the shape factor. When $n = 0$, Eq. 1 corresponds to the parallel transport (i.e., along parallel pore paths) of penetrants through MMMs and can be expressed as

$$P_{\text{eff}} = (1-\phi_d)P_c + \phi_d P_d \quad (2)$$

When $n = 1$, Eq. 1 corresponds to the serial transport (i.e., along a series of pore paths) of penetrants through MMMs and can be expressed as

$$P_{\text{eff}} = \frac{P_c P_d}{P_d(1-\phi_d) + \phi_d P_c} \quad (3)$$

When $n = 1/3$[21], Eq. 1 corresponds to the most general cases for MMMs and is known as Maxwell equation which is as follows:

$$P_{\text{eff}} = P_c \left[\frac{P_d + 2P_c - 2\phi_d(P_c - P_d)}{P_d + 2P_c + \phi_d(P_c - P_d)} \right] \quad (4)$$

Generally, it is assumed in the Maxwell model that the transport of gas penetrants around the filler particles is not affected by the presence of nearby particles. Hence, it is suggested that the Maxwell model can give good predictions only on MMMs with low filler loadings in which the interparticle distance is sufficiently large to ensure that the flow patterns around any one particle is undisturbed by the presence of others.

In this study, as P_d for PVDF/SiO_2 MMMs is 0 for the nonporous SiO_2 filler, the Maxwell Eq. 4 becomes

$$P_{\text{eff}} = P_c \frac{2 - 2\phi_d}{2 + \phi_d} \quad (5)$$

For PVDF/MCM-41 MMMs, the pores of the MCM-41 are mesoporous and therefore P_d is much larger than P_c. This condition will also be applied to the subsequent Higuchi, Bruggeman, and Bottcher-Landauer models presented here. The Maxwell Eq. 4 can then be written as

$$P_{\text{eff}} = P_c \frac{1+2\phi_d}{1-\phi_d} \tag{6}$$

For PVDF/4A MMMs, the permeabilities of He and CO_2 can still be calculated using Eq. 6 as the diameters of the He and CO_2 molecules are smaller than the pore sizes of the zeolite 4A powder and therefore $P_d >> P_c$. However, the calculations of the permeabilities of O_2 and N_2 have to be strictly based on Eq. 4 as the diameters of the O_2 and N_2 molecules are much closer to the pore size of the zeolite 4A powder and therefore P_d and P_c have the same order of magnitude. These conditions will also be applied to the subsequent Higuchi, Bruggeman, and Bottcher-Landauer models presented here.

Higuchi *model*

Higuchi proposed another model as given in Eq. 7 to estimate the permeability of MMMs.[3,8] The Higuchi model[3,8] is applied for random dispersion of spherical filler particles but lacks the well-defined mathematical rigor.

$$P_{\text{eff}} = P_c \left[1 + \frac{3\phi_d}{\frac{P_d+2P_c}{P_d-P_c} - \phi_d - K\left[\frac{(1-\phi_d)(P_d-P_c)}{P_d+2P_c}\right]} \right] \tag{7}$$

where K is an empirical constant and is generally assigned a value of 0.78 on the basis of experimental data. Higuchi indicated that the value of K is exaggerated by an "asphericity factor." However, no physical basis could be attributed to K.

For PVDF/SiO_2 MMMs, as P_d is equal to 0 for the nonporous SiO_2 powder, the Higuchi model, that is, Eq. 7, becomes

$$P_{\text{eff}} = P_c \left[1 - \frac{6\phi_d}{3.22+2.78\phi_d} \right] \tag{8}$$

For PVDF/MCM-41 MMMs, as $P_d >> P_c$ for mesoporous MCM-41, the Higuchi model, that is, Eq. 7, can be approximately written as

$$P_{\text{eff}} = P_c \left[\frac{0.22+2.78\phi_d}{0.22-0.22\phi_d} \right] \tag{9}$$

For PVDF/4A MMMs, the permeabilities of He and CO_2 can be calculated using Eq. 9 due to the fact that $P_d >> P_c$. However, the calculations of the permeabilities of O_2 and N_2 have to be based on Eq. 7.

Bruggeman model

Based on the effective medium theory, Bruggeman derived Eq. 10 to estimate the permeability of MMMs.[21] Due to the fact that the effective medium theory treats the local permeability as fluctuations about the effective permeability of an uniform medium, no distinction between continuous phase and dispersed phase is made. In contrast to the Maxwell model, the Bruggeman model considers the effects of the presence of nearby particles on the transport of gases around filler particles by introducing an asymmetrical integration technique. Therefore, the Bruggeman model,[21] which is particularly recommended for high filler loadings, is as follows:

$$\left(\frac{P_d}{P_c} - \frac{P_{\text{eff}}}{P_c}\right)\left(\frac{P_c}{P_{\text{eff}}}\right)^{1/3} = (1-\phi_d)\left(\frac{P_d}{P_c} - 1\right) \tag{10}$$

Equation 10 is a third order algebraic expression in P_{eff}.

For PVDF/SiO_2 MMMs, as P_d equals to 0 and the Bruggeman model, that is, Eq. 10, will be simplified to

$$P_{\text{eff}} = P_c (1-\phi_d)^{3/2} \tag{11}$$

For PVDF/MCM-41 MMMs, as $P_d >> P_c$, the Bruggeman model, that is, Eq. 10, can be approximately simplified to

$$P_{\text{eff}} = \frac{P_c}{(1-\phi_d)^3} \tag{12}$$

For PVDF/4A MMMs, the permeabilities of He and CO_2 can be calculated using Eq. 12 due to the fact that $P_d >> P_c$. However, the calculations of the permeabilities of O_2 and N_2 have to be based on Eq. 10.

Bottcher-Landauer model

Bottcher-Landauer model was originally developed to calculate the electrical resistance of binary metallic mixtures and subsequently analogously applied to estimate the permeability of MMMs.[3,8] The Bottcher-Landauer model[3,8] is

$$\left(\frac{P_d}{P_c} + \frac{2P_{\text{eff}}}{P_c}\right)\left(1 - \frac{P_c}{P_{\text{eff}}}\right) = 3\phi_d\left(\frac{P_d}{P_c} - 1\right) \tag{13}$$

Equation 13 is a second order algebraic expression in P_{eff}.

For PVDF/SiO_2 MMMs, as P_d equals to 0 and the Bottcher-Landauer model, that is, Eq. 13, becomes

$$P_{\text{eff}} = P_c (2-3\phi_d)/2 \tag{14}$$

For PVDF/MCM-41 MMMs, as $P_d >> P_c$, the Bottcher-Landauer, that is, Eq. 13, can be simplified to

$$P_{\text{eff}} = \frac{P_c}{(1-3\phi_d)} \tag{15}$$

For PVDF/4A MMMs, the permeabilities of He and CO_2 can be calculated using Eq. 15 due to the fact that $P_d >> P_c$. However, the calculations of the permeabilities of O_2 and N_2 have to be based on Eq. 13.

Modified Maxwell model

Moore and Koros[10] observed some nonideal behaviors of MMMs induced by interface voids, polymer chain rigidifications, and pore blockages, and they modified the Maxwell equation with reference to the polymer/inorganic interface properties. Considering the influence of interface voids in MMMs, a three-phase system consisting of the inorganic filler phase, polymer phase, and the interface voids was proposed. The permeability P_{3MM} of the three-phase membrane is obtained by applying the Maxwell model twice. First, gas flows through the interface voids by Knudsen diffusion which is modified slightly to account for the finite size of the gas molecules and this Knudsen diffusion coefficient D_{AK}[10] is given by Eq. 16.

$$D_{AK} = 9.7\times10^{-5} r \sqrt{\frac{T}{M_A}}\left[1 - \frac{d_g}{2r}\right] \tag{16}$$

where r is the effective pore radius, T is the temperature, M_A is the molecular weight, and d_g is the gas molecular size.

The solubility coefficient S_v[10] in these voids is assumed to be that in the gas phase, that is

$$S_V = \frac{1}{RT}\left(1-\frac{d_g}{2r}\right)^2 \tag{17}$$

where R is the gas constant.

The gas permeability P_v[10] through the voids is the product of D_{AK} and S_v such that

$$P_v = \frac{9.7\times10^{-5}r}{RT}\sqrt{\frac{T}{M_A}}\left[1-\frac{d_g}{2r}\right]^3 \tag{18}$$

Second, a modified Maxwell equation is used to obtain the permeability of the combined interface voids and inorganic phase with the interface void as the continuous phase and the inorganic phase as the dispersed phase. This modified Maxwell equation[10] is

$$P_{eff} = P_v\left[\frac{P_d+2P_v-2\phi(P_v-P_d)}{P_d+2P_v+\phi(P_v-P_d)}\right] \tag{19}$$

where

$$\phi = \frac{V_f}{V_f+V_v} \tag{20}$$

Here, P_{eff} is the permeability of the combined dispersed or inorganic phase and interface void, P_d is the permeability of the dispersed or inorganic phase, P_v is the permeability of the interface voids, V_f and V_v are the volumes of inorganic filler and voids, respectively.

Finally, the value of the permeability of the combined filler and interface void, P_{eff}, can then be used along with the continuous polymer phase permeability, P_c, to obtain a predicted permeability P_{3MM} for the three-phase MMMs by applying the Maxwell equation a second time.[10]

$$P_{3MM} = P_c\left[\frac{P_{eff}+2P_c-2\phi'(P_c-P_{eff})}{P_{eff}+2P_c+\phi'(P_c-P_{eff})}\right] \tag{21}$$

where

$$\phi' = \frac{V_f+V_v}{V_f+V_v+V_p} \tag{22}$$

and V_p is the polymer volume.

If $P_{eff} >> P_c$, the permeability P_{3MMM} for the three-phase MMMs becomes

$$P_{3MM} = P_c\times\frac{1+2\phi'}{1-\phi'} \tag{23}$$

Assuming that the inorganic particles are perfectly spherical and the voids are distributed evenly around the particles, Eqs 20 and 22 can be respectively expressed as

$$\phi = \frac{r^3}{(r+l)^3} = \frac{1}{(1+l/r)^3} \tag{24}$$

and

$$\phi' = \frac{\phi_f^N}{\phi_f^N+\frac{1-\phi_f^N}{(1+l/r)^3}} \tag{25}$$

where $\phi_f^N$is the inorganic nominal volume fraction, r is the particle size, and l is the void thickness. ϕ_f^N is defined as

$$\phi_f^N = \frac{V_f}{V_f+V_p} \tag{26}$$

By substituting Eqs. 24 and 25, the void volume fraction $\phi_V$can be estimated as follows

$$\phi_v = \frac{V_v}{V_v+V_f+V_p} = \frac{(l/r+1)^3-1}{(l/r+1)^3+\frac{1-\phi_f^N}{\phi_f^N}} \tag{27}$$

The void volume fraction of the MMM can also be calculated as follows[22]

$$\phi_V = \frac{\rho_t-\rho_m}{\rho_t} \tag{28}$$

where ρ_t and ρ_m are the theoretical and measured densities of the MMMs, respectively.

Using Eqs. 27 and 28, the relationship between l and r can be obtained as follows

$$l = \left[\left(\frac{a\left(1-\phi_f^N\right)+1}{1-a\phi_f^N}\right)^{1/3}-1\right]\times r \tag{29}$$

where a is the gradient of the line for the void volume fraction ϕ_V vs. the inorganic filler nominal volume fraction ϕ_f^N. Hence, using this derived expression, the void thickness of the MMM can be determined if the experimental determined values of a, ϕ_f^N, and r are known.

Extended modified Maxwell model for PVDF MMMs

It has been known that the permeability of PVDF matrix is closely related to its crystallinity. Generally, crystalline polymer structure can influence the permeability of polymer membranes in two ways. Crystallinity will decrease the solubility coefficient due to the fact that the crystalline polymer with closing packing density exhibits lower solubility compared with that of amorphous polymer. The relationship[13] can be expressed as

$$S = S^*\times\alpha \tag{30}$$

where S and S^* are the solubility coefficients of semicrystalline polymer and amorphous polymer, respectively, and α is the amorphous polymer fraction. In addition, the crystalline polymer chains also block the diffusion of gas penetrants and decrease the diffusion coefficient, and the relationship is given by

$$D = D^*\times\alpha \tag{31}$$

where D and D^* are the diffusion coefficients of semicrystalline polymer and amorphous polymer, respectively. The permeability coefficient P is the product of solubility coefficient and diffusion coefficient and is given as

$$P = S^*\times D^*\times\alpha^2 = P^*\times\alpha^2 \tag{32}$$

where P^* is the permeability coefficient of the amorphous polymer and P here will represent Pc in Eq. 21.

Usually, the presence of crystalline polymer will influence the transport properties of the surrounding amorphous polymers. An immobilization factor, β, is used to represent the degree of tautness in the intercrystalline amorphous segments. Hence

$$P = P^*\alpha^2/\beta \tag{33}$$

Finally, with the effects of crystallinity and immobilization factor taken into consideration, the permeability P in

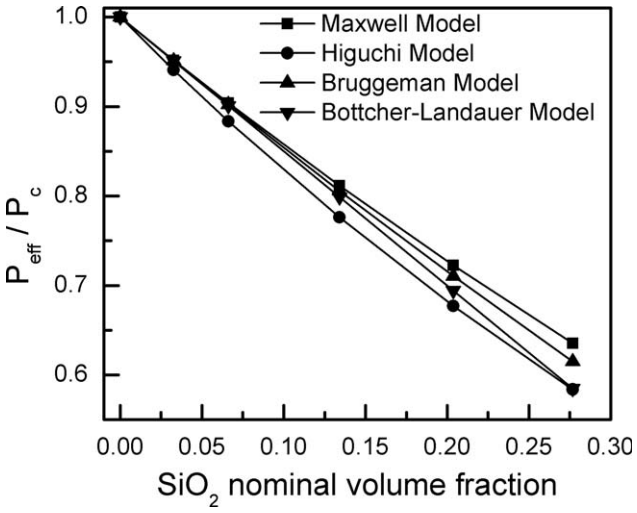

Figure 1. Permeability model results of PVDF/SiO_2 MMMs as a function of SiO_2 nominal volume fraction.

Eq. 33 is used for *Pc* in Eq. 21 to form the extended modified Maxwell model. Consequently, the permeability of PVDF matrix is dependent on the filler content because its crystallinity is related to the filler content. According to El-Hibri and Paul,[13] the permeabilities of complete amorphous PVDF, P^*, for He, CO_2, O_2, and N_2 were 7.16, 2.15, 0.344, and 0.093 Barrer, respectively. The immobilization factor, β, of crystalline polymer is dependent on the gas penetrant molecular size. The β values are set to be 1.0, 1.2, 1.4, and 1.5 for He, CO_2, O_2, and N_2, respectively.[13,23] The volume fraction of the amorphous polymer, α, can be determined by the crystallinity χ of the MMMs as follows

$$\alpha = 1 - \chi \tag{34}$$

Supplementary information on the permeability of MCM-41 particles, diffusion and solubility coefficients for zeolite 4A are given in Appendix A.

Results and Discussion

Relative gas (He, CO_2, O_2, and N_2) permeabilities P_{eff}/P_c (ratio of permeability of MMM to that of polymer membrane) of PVDF/SiO_2 MMMs based on the Maxwell model, Higuchi model, Bruggeman model, and Bottcher-Landauer model for varying volume fractions are shown in Figure 1. Due to the nonporous nature of the fumed SiO_2 particles, the permeabilities of PVDF/SiO_2 MMMs predicted by all four models were smaller than that of pure PVDF membrane and monotonically decreased with increasing SiO_2 nominal volume fraction. This is to be expected due to decreasing polymer content for gas dissolution and diffusion as the SiO_2 volume fraction increases. Among these four models, the Maxwell model predicted the largest values while the Higuchi model resulted in the lowest values of gas permeabilities and the values given by the Bruggeman model and the Bottcher-Landauer model lied between those of the two preceding models. The permeability values followed this order: Maxwell model > Bruggeman model > Bottcher-Landauer model > Higuchi model. Due to the nonporous properties of SiO_2, P_d equals to zero in the PVDF/SiO_2 MMMs. These models except the Maxwell model lack the well-defined physical basis and make some approximations to treat the complexity of the MMMs. For instance, the Bruggeman model considers the effects of the presence of nearby particles on the transport of gases around the filler particles by introducing an asymmetric integration technique. However, for the nonporous SiO_2 particles, no path is available for the transport of gases through the dense particles. For the Higuchi model, the assigned value of 0.78 for the empirical constant K might not be appropriate for the SiO_2 particles. For the Bottcher-Landauer model, it was developed to calculate the electrical resistance of binary metallic mixtures and therefore the predicted permeabilities of MMMs are only approximate. These approximations could lead to the lower predicted permeability values.

In contrast to nonporous SiO_2, mesoporous MCM-41 exhibited much higher permeabilities than that of pure PVDF. In Figure 2, the relative permeabilities P_{eff}/P_c of PVDF/MCM-41 MMMs predicted by all four models were higher than that of pure PVDF membrane and the permeability increased with increasing MCM-41 nominal volume fraction due to increasing pores. The permeability values for PVDF/MCM-41 MMMs given by the Maxwell model were the smallest while those given by the Higuchi model were the greatest. The order of permeability values was the reversed order to PVDF/SiO_2 MMMs. This reversed trend—Higuchi model > Bottcher-Landauer model > Bruggeman model > Maxwell model, has indicated the increasing dominance of the volume fraction of the MCM-41, ϕ_d, on the overall MMM permeability, P_{eff}, in the models in this sequence. The curves based on Maxwell, Bruggeman, and Higuchi models showed an approximate linear relationship between permeability and MCM-41 nominal volume fraction while the curve based on Bottcher-Landauer model exhibited an exponential relationship between permeability and MCM-41 nominal volume fraction due to the predominance of ϕ_d on permeability in the Bottcher-Landauer model.

The permeability values of PVDF/SiO_2 and PVDF/MCM-41 MMMs based on the four models were consistent for all the test gases given that the SiO_2 particles were nonporous and the MCM-41 particles were of pore size of 2.7 nm. These two inorganic fillers showed no selectivities for He, CO_2, O_2, and N_2. On the basis of the four models, the

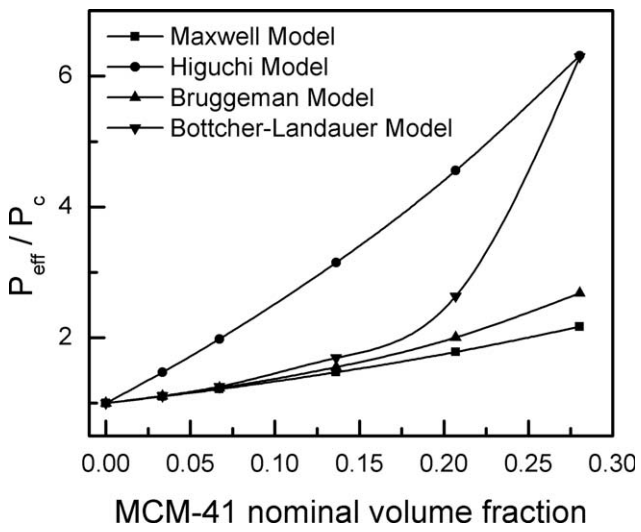

Figure 2. Permeability model results of PVDF/MCM-41 MMMs as a function of MCM-41 nominal volume fraction.

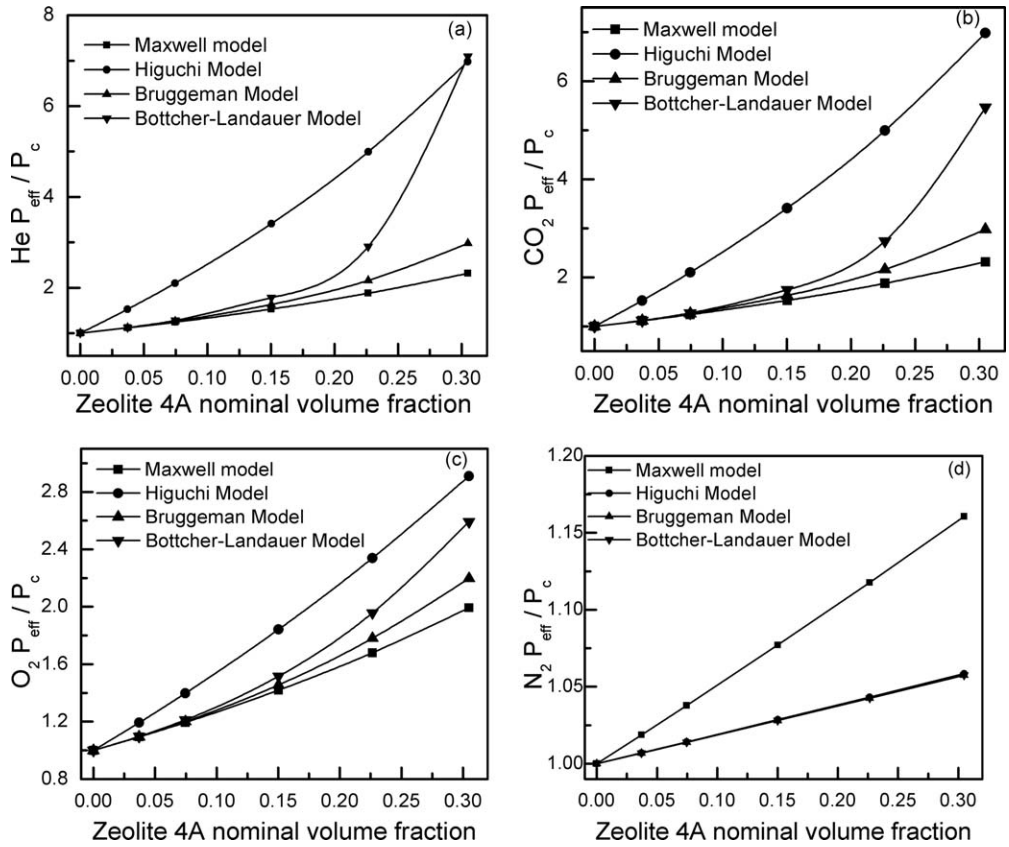

Figure 3. Permeability model results of PVDF/4A MMMs as a function of zeolite 4A nominal volume fraction for (a) He, (b) CO_2, (c) O_2, and (d) N_2.

additions of SiO_2 and MCM-41 into PVDF would only affect the permeabilities of the MMMs but their selectivities would be the same as that of the pure PVDF membrane. These results were not manifested for the PVDF/4A MMMs because zeolite 4A particles produced different permeabilities of O_2 and N_2 with the PVDF matrix and consequently resulted in a high selectivity for these two gases. The He and CO_2 permeabilities of PVDF/4A MMMs based on the four models are shown in Figures 3a and b, respectively, which were very similar to those of PVDF/MCM-41 MMMs due to the much higher He and CO_2 permeabilities through the zeolite 4A particles than through the PVDF matrix. As the molecule size of the penetrants increased in the following order: He (2.6Å) >CO_2 (3.3 Å) >O_2 (3.46 Å) >N_2 (3.64 Å) with its respective molecular gas diameter given within the parenthesis, the zeolite 4A particles exhibited higher permeabilities of He and CO_2 as compared with those of O_2 and N_2. For PVDF/4A MMMs, the order of magnitude of O_2 permeability (Figure 3 c) was similar to those of He and CO_2: the permeability values given by the Higuchi model were the largest while those given by the Maxwell model were the smallest, and the values given by Bottcher-Landauer and Bruggeman models lied between the four models. However, the differences in the O_2 permeability values given by the four models narrowed as the four curves became closer. The N_2 permeabilities (Figure 3 d) of PVDF/4A MMMs for the four models showed different characteristics. The N_2 permeability values given by the Maxwell model were the largest while the values given by the other three curves collapsed together.

Overall, the shape of the permeability curves of the MMMs given by the models is determined by the two parameters, that is, the filler volume fraction and the relative permeability P_d/P_c. Given that all the test gases (He, CO_2, O_2, and N_2) for the PVDF/SiO_2 MMMs, $P_d \ll P_c$ whereas for the PVDF/MCM-41 MMMs, $P_d \gg P_c$. Therefore, the order of the permeability values of PVDF/SiO_2 MMMs given by the four models was exactly the reverse of those of the PVDF/MCM-41 MMMs. For the PVDF/4A MMMs, the relative permeability P_d/P_c is dependent on the type of test gas. For He and CO_2, $P_d \gg P_c$, the results were of similar trends to the PVDF/MCM-41 MMMs. However, for O_2 and N_2, P_c is comparable to P_d, and this led to significant variations of the permeability curves for varying inorganic filler volume fractions.

Maxwell, Higuchi, Bottcher-Landauer, and Bruggeman models ideally treat the MMMs as two phases, that is, polymer matrix phase and inorganic filler phase. In this study, three inorganic fillers SiO_2, MCM-41 and zeolite 4A were used without any modifications; these fillers are hydrophilic and show poor compatibility with the PVDF matrix. It is reasonable to assume that some voids may be present between the particle–polymer interfaces and this assumption can be verified if the theoretical density differs from the experimental density.

Based on Eqs. 18 and 29, the gas permeability through the voids is highly dependent on the void thickness as shown in Figure 4. The O_2 permeability through the voids increased steeply with increasing void thickness and this upward trend gradually slowed down as the void thickness was greater

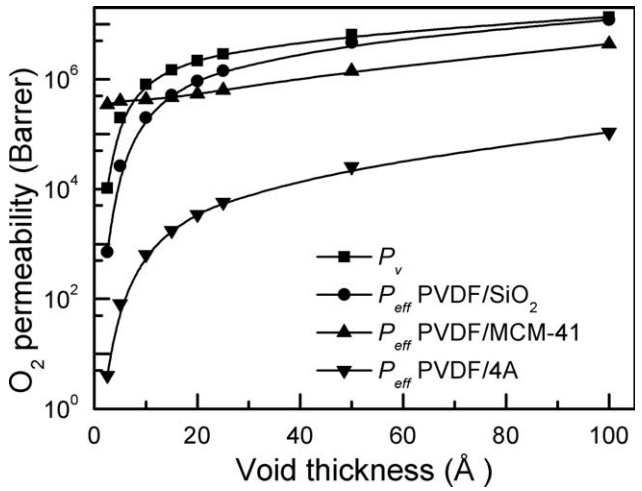

Figure 4. P_{eff} of PVDF/SiO_2, PVDF/MCM-41, PVDF/4A MMMs, and P_v as a function of void thickness.

than 30 Å. The O_2 permeability, P_{eff}, of the MMMs based on Eq. 19 is also shown in Figure 4. For PVDF/SiO_2 and PVDF/4A MMMs, the O_2 permeability, P_{eff}, showed a similar trend as P_v except that P_{eff} was smaller than P_v for the same void thickness. For PVDF/MCM-41 MMMs, the O_2 permeability, P_{eff}, increased linearly with increasing void thickness. In using the modified Maxwell model, the P_{eff} value based on the Eq. 19 is much greater than the permeability P_c of PVDF even though the void thickness is as small as 2.5 Å. The fact that P_{eff} is much larger than P_c in Eq. 21 for all the three MMMs enables the calculations of the permeability, P_{3MM}, of MMMs using Eq. 23.

The permeability results given by the modified Maxwell model are shown in Figures 5a–c, in which five, six, and seven different void thicknesses are plotted for PVDF/SiO_2, PVDF/MCM-41, and PVDF/4A MMMs, respectively. For all the MMMs, the permeabilities were highly dependent on the void thickness and the inorganic filler nominal volume fraction. For smaller void thickness, the permeabilities showed an approximate linear relationship with the nominal inorganic filler volume fraction while for larger void thickness, a nonlinear relationship was observed. For the same nominal volume fraction, the permeability increased with increasing void thickness and the effect of void thickness on the permeability was much more significant for the PVDF/SiO_2 MMM than the PVDF/MCM-41 and PVDF/4A MMMs. For instance, the largest P_{3MM}/P_{eff} value for PVDF/28% SiO_2 MMM was 17.5 for a void thickness of 10 nm while the largest P_{3MM}/P_{eff} value for PVDF/28% MCM-41 and PVDF/30.5% 4A MMMs were 26.2 and 8.6 for void thicknesses of 100 and 2000 nm, respectively. This indicated that the larger inorganic fillers, that is, zeolite 4A and MCM-41 with particle sizes of 2.5 μm and 56 nm, respectively, exhibited better tolerance with voids than the smaller inorganic filler, that is, SiO_2 with particle size of 7 nm. This is due to the fact that for the same void thickness, MMM with an inorganic filler of a larger particle size has a lower void volume fraction.

Figure 5 shows that the void thickness is a critical parameter but it is assumed to be independent of the nominal inorganic filler volume fraction in the modified Maxwell model. On the contrary, the void thickness is dependent on the properties of the inorganic filler including its particle size, its surface properties and its nominal volume fraction in the resulting MMMs and is closely related to the void fraction. The void volume fraction of the MMMs can be calculated using Eq. 28.[22]

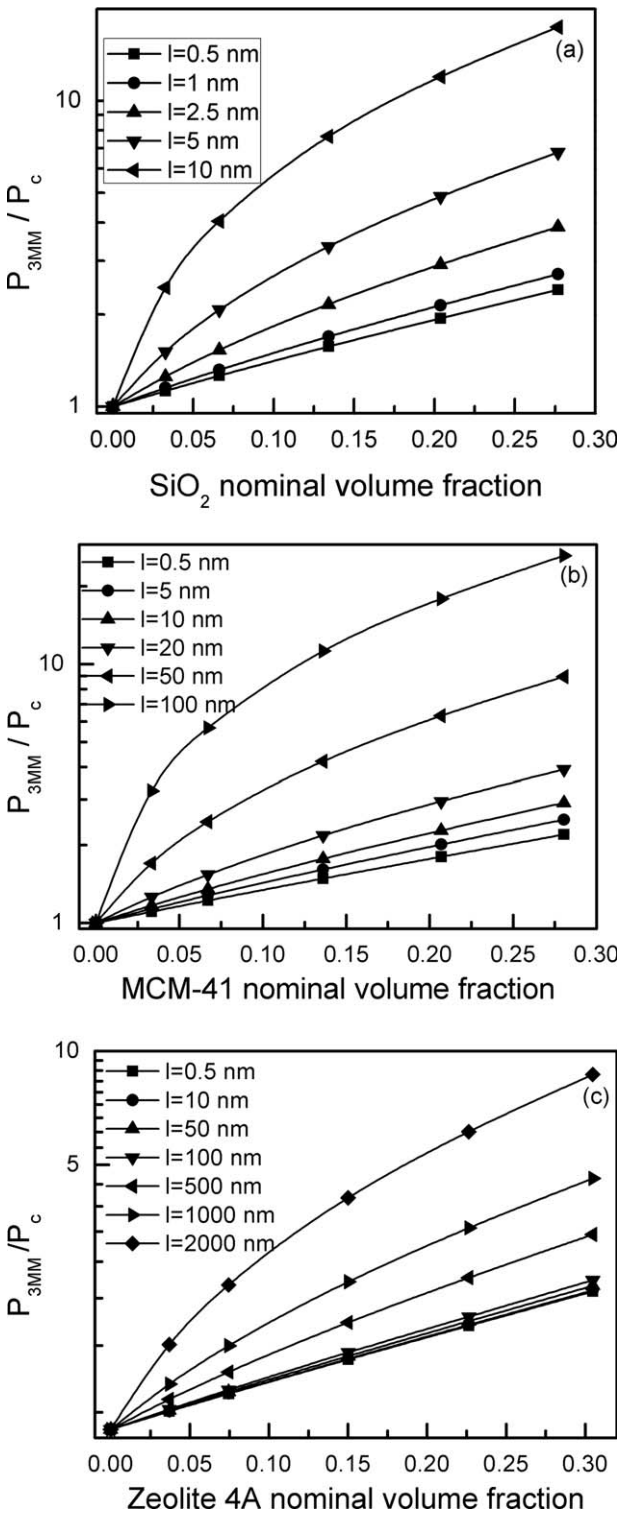

Figure 5. Permeability model results based on modified Maxwell equation for (a) PVDF/SiO_2, (b) PVDF/MCM-41, and (c) PVDF/4A as a function of the inorganic filler nominal volume fraction.

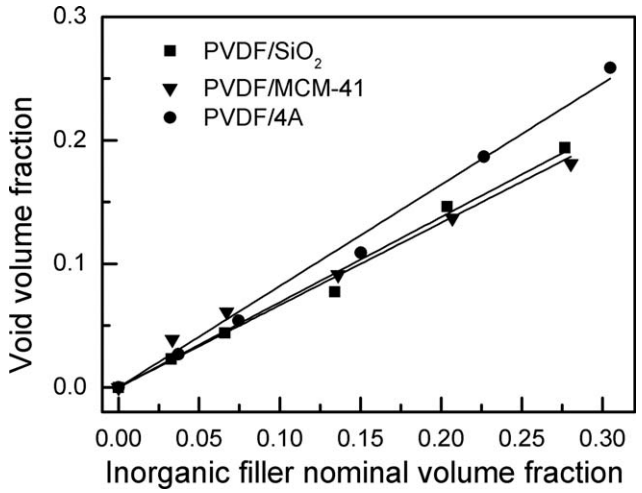

Figure 6. Void volume fraction as a function of inorganic filler nominal volume fraction.

Figure 6 shows the relationship between the void fraction and the inorganic filler nominal volume fraction. The void volume fraction of PVDF/MCM-41 and PVDF/4A shown in Figure 6 were obtained after subtracting the pore volumes of MCM-41 and zeolite 4A, respectively. With the same inorganic filler nominal volume fraction, PVDF/SiO_2 and PVDF/MCM-41 MMMs had similar void fractions which were smaller than that of PVDF/4A MMMs. Using linear fits, the slopes of the curves were 0.69, 0.67, and 0.82 for PVDF/SiO_2, PVDF/MCM-41, and PVDF/4A MMMs, respectively. Subsequently, the void thickness was estimated using Eq. 29 and the results are presented in Figure 7. For the three types of MMMs, the void thickness increased with increasing inorganic filler nominal volume fraction. However, the void thickness showed significant differences due to the different particle sizes of the inorganic fillers, which is supported by Eq. 29.

From the DSC measurements, the crystallinity of the resulting MMM was determined. Figure 8 shows the amorphous polymer fraction, α, as a function of the inorganic filler nominal volume fraction. For the three types of MMMs, the addition of inorganic filler increased the crystallinity of the PVDF matrix due to the inorganic fillers acting as nucleation agents during the crystallization of PVDF. The amorphous polymer volume fraction decreased sharply with the addition of inorganic filler of 0.03 volume fraction and this downward trend slowed down, forming nearly plateaus for further additions of the inorganic fillers.

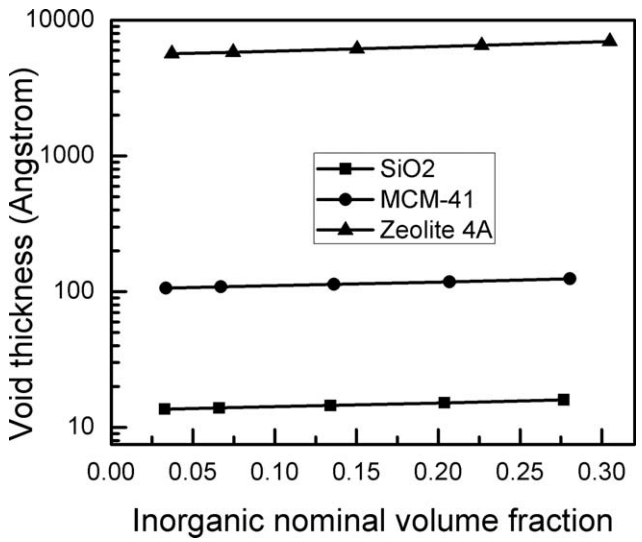

Figure 7. Void thickness as a function of inorganic nominal volume fraction for PVDF/SiO_2, PVDF/MCM-41, and PVDF/4A.

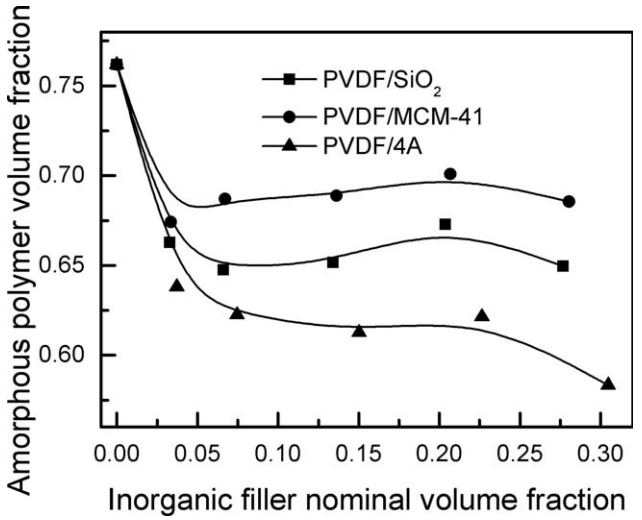

Figure 8. Amorphous polymer volume fraction as a function of inorganic filler nominal volume fraction.

The experimental and modeling results for the permeabilities of the three types of MMMs were compared and shown in Figure 9. The solid symbols denote the experimental results while the dashed lines represent the modified Maxwell model based on Eq. 21. In addition, the present model results (solid lines) were derived from the extended modified Maxwell model presented herein in which the effects of crystallinity and the immobilization factor β of the PVDF polymer were considered. In these two models, the void thickness of the MMMs was calculated in order to determine the permeability of the MMM. Pure PVDF membrane had experimental permeabilities of 3.94, 1.18, 0.14, and 0.04 Barrer which were very consistent with the modeling results of 3.78, 1.18, 0.14, and 0.04 Barrer for He, CO_2, O_2 and N_2, respectively, for the two models. Unexpectedly, the experimental permeability results showed no significant differences among the PVDF/SiO_2, PVDF/MCM-41, and PVDF/4A MMMs although the inorganic fillers that is, SiO_2, MCM-41 and 4A, had different properties such as particle size and pore structure. This behavior could be attributed to the fact that the gas penetrants bypassed the inorganic filler particles in the MMMs altogether due to the presence of voids, resulting in negligible passage through the inorganic fillers. For all the three MMMs, the permeabilities initially decreased when the inorganic fillers were about 4 wt% and then increased with further increases in the inorganic filler content, resulting in minimum values for the MMMs with 4 wt% inorganic fillers. This behavior can be explained as follows. On one hand, the permeabilities of the MMMs increased with increasing inorganic fillers due to the formation of voids.[24] Conversely, the addition of the inorganic filler could lead to increase in the crystallinity of the PVDF matrix, which could in turn decrease the permeability of the

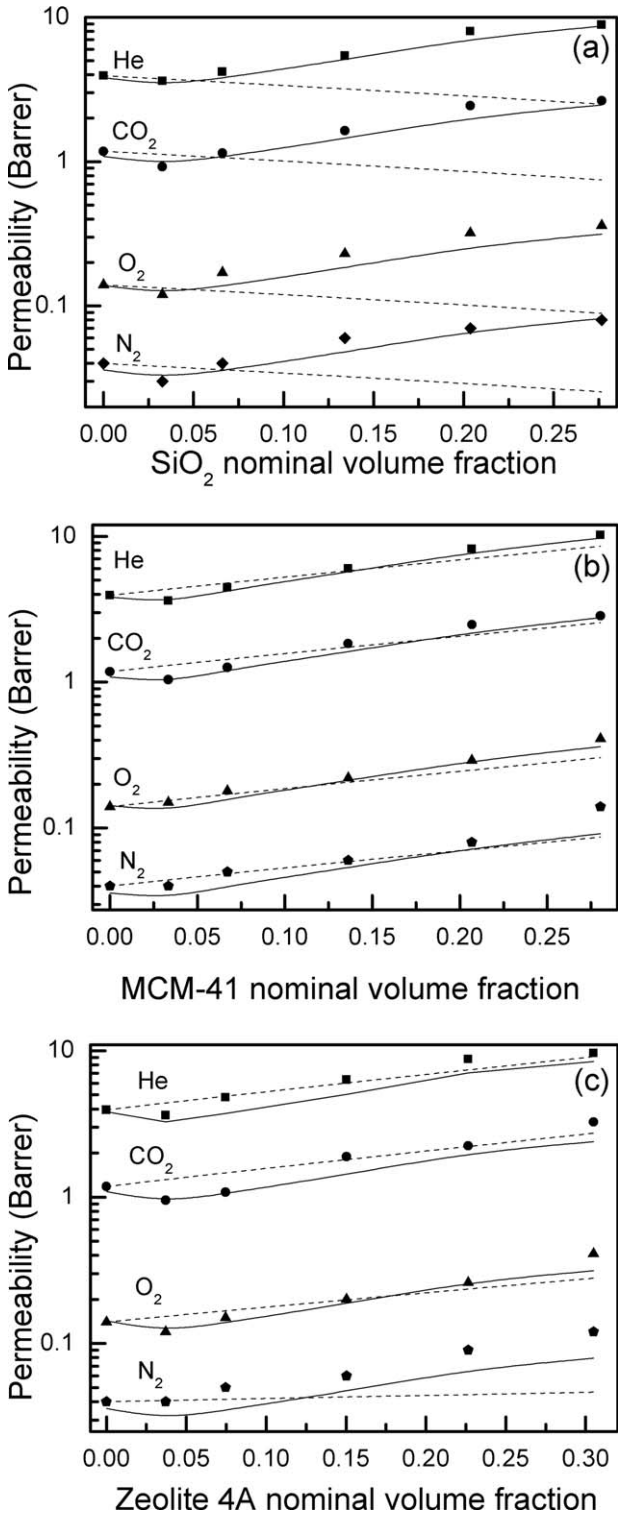

Figure 9. Permeability results for (a) PVDF/SiO_2, (b) PVDF/MCM-41, and (c) PVDF/4A MMMs (solid symbols: experimental results; — present modeling curve; —— modified Maxwell modeling curve, Eq. 21).

MMM. Generally, the permeability model results as predicted by the extended modified Maxwell model had better agreement with the experimental permeability results than the modified Maxwell model, especially for the case of PVDF/SiO_2 MMM. Unexceptional large deviations between the modified Maxwell model results and the experimental permeability results were clearly evident for the PVDF/SiO_2 MMM. In essence, the effects of crystallinity and immobilization factor have to be considered in the modified Maxwell model for PVDF MMMs. The discrepancy as observed by the small deviations between the experimental permeability results and the modeling permeability results as predicted by the extended modified Maxwell model was attributed to two factors: (1) the formation of filler particle aggregates, particularly for the nano-SiO_2 particles with the smallest size, which was not taken into consideration in the modeling work and (2) the assumption that the filler particles were perfectly spheres. From the permeability results in Figure 9, the theoretical selectivities of various gas combinations such as H_2/N_2, CO_2/N_2, or O_2/N_2 could be calculated. It was found that the selectivities of PVDF/SiO_2, PVDF/MCM-41, and PVDF/4A MMMs were almost the same as those of pure PVDF membrane. The reason for this behavior is again that the gas penetrants bypassed the inorganic filler particles due to the presence of voids.

Sample calculations relating to the use of the various models for the P84/SiO_2 composite membranes are given in Appendix B

Conclusions

The permeabilities of the PVDF/SiO_2, PVDF/MCM-41, and PVDF/4A MMMs were modeled using Maxwell, Higuchi, Bottcher-Landauer, Bruggeman, and modified Maxwell models. For PVDF/SiO_2 MMMs, the permeability model results followed the following order: Maxwell model>Bruggeman model>Bottcher-Landauer model>Higuchi model, which was different for that of PVDF/MCM-41 MMMs. Based on these four models, the additions of SiO_2 and MCM-41 only changed the permeability but the selectivity would remain the same as the polymer matrix. For the PVDF/4A MMMs, the He and CO_2 permeabilities showed similar trends with those of PVDF/MCM-41 MMMs while the N_2 and O_2 permeabilities showed different trends for the two MMMs. The permeability values of the modified Maxwell model were highly dependent on the void thickness. For all the three MMMs, the permeabilites increased with increasing void thickness and this upward trend was particularly significant for the PVDF/SiO_2 MMMs due to the smaller particle size of SiO_2. Based on the relationship between the void volume fraction and the inorganic filler nominal volume fraction, it was possible to estimate the void thickness. Unexpectedly, the experimental permeability results of the MMMs showed no significant differences for the three types of MMMs; the permeabilities decreased initially as the inorganic fillers was about 4 wt% and then subsequently increased with further increases in the inorganic filler content. Using the extended modified Maxwell model and taking into account the crystalline effect and the immobilization factor on the permeability, the permeability modeling results matched the experimental permeability results reasonably well, indicating the success of capturing the gas transport phenomena of MMMs, and thereby showing the inadequacies of the Maxwell, Higuchi, Bottcher-Landauer, and Bruggeman models. Due to poor compatibility between the filler particles and the polymer chains, the gas penetrants mainly transport through the voids, resulting in increasing permeability for increasing volume fraction of the inorganic filler.

Notation

a = gradient of line for void volume fraction vs. filler volume fraction
D = diffusion coefficient of semicrystalline polymer
D^* = diffusion coefficient of amorphous polymer
D_{AK} = diffusion coefficient of voids, cm^2/s
d_g = gas molecular diameter, Å
l = void thickness, Å
M_A = molecular weight, g/mol
n = structure factor
P = permeability of polymer matrix, Barrer
P^* = permeability of amorphous polymer, Barrer
P_{3MM} = permeability of the three-phase MMMs, Barrer
P_c = permeability of continuous phase, Barrer
P_d = permeability of dispersed phase, Barrer
P_{eff} = effective permeability of two phases, Barrer
P_v = permeability of voids, Barrer
R = universal gas constant
r = effective pore radius or particle size, Å
S = solubility coefficient of semicrystalline polymer
S_v = solubility coefficient, mol Pa^{-1} s^{-1}
S^* = solubility coefficient of amorphous polymer
T = absolute temperature, K
V_f = volume of inorganic fillers
V_p = volume of polymer
V_v = volume of voids
α = amorphous polymer fraction
β = immobilization factor
ρ_m = measured density, g/cm^3
ρ_t = theoretical density, g/cm^3
ϕ = volume fraction of filler in the combined inorganic phase and void phase
ϕ' = volume fraction of inorganic filler and voids
ϕ_d = volume fraction of dispersed phase
ϕ_f^N = inorganic filler nominal volume fraction
ϕ_v = void volume fraction

Literature Cited

1. Chung TS, Jiang LY, Li Y, Kulprathipanja S. Mixed matrix membranes (MMMs) comprising organic polymers with dispersed inorganic fillers for gas separation. *Prog Poly Sci*. 2007;32:483–507.
2. Mahajan R, Koros WJ. Factors controlling successful formation of mixed-matrix gas separation materials. *Ind Eng Chem Res*. 2000;39:2692–2696.
3. Mahajan R, Koros WJ. Mixed matrix membrane materials with glassy polymers. Part 1. *Poly Eng Sci*. 2002;42:1420–1431.
4. Mahajan R, Koros WJ. Mixed matrix membrane materials with glassy polymers. Part 2. *Poly Eng Sci*. 2002;42:1432–1441.
5. Mahajan R, Burns R, Schaeffer M, Koros WJ. Challenges in forming successful mixed matrix membranes with rigid polymeric materials. *J Appl Poly Sci*. 2002;86:881–890.
6. Robeson LM. Correlation of separation factor versus permeability for polymeric membranes. *J Membr Sci*. 1991;62:165–185.
7. Robeson LM. The upper bound revisited. *J Membr Sci*. 2008;320:390–400.
8. Petropoulos JH. A comparative study of approaches applied to the permeability of binary composite polymeric materials. *J Poly Sci Poly Phys*. 1985;23:1309–1324.
9. Senuma A. Generalized equation for the permeability of heterogeneous polymer materials. *Macromol Chem Phys*. 2001;202:1737–1742.
10. Moore TT, Koros WJ. Non-ideal effects in organic–inorganic materials for gas separation membranes. *J Mol Struct*. 2005;739:87–98.
11. McGonigle EA, Liggata JJ, Pethrick RA, Jenkins SD, Daly JH, Hayward D. Permeability of N2, Ar, He, O2 and CO2 through biaxially oriented polyester films-dependence on free volume. *Polymer* 2001;42:2413–2426.
12. Polyakova A, Stepanov EV, Sekelik D, Schiraldi DA, Hiltner A, Baer E. Effect of crystallization on oxygen-barrier properties of copolyesters based on ethylene terephthalate. *J Polym Sci Part B: Polym Phys*. 2001;39:1911–1919.
13. El-Hibri MJ, Paul DR. Gas transport in poly(viny1idene fluoride): effects of uniaxial drawing and processing temperature. *J Appl Poly Sci*. 1986;31:2533–2560.
14. Wang KY, Foo SW, Chung TS. Mixed matrix PVDF hollow fiber membranes with nanoscale pores for desalination through direct contact membrane distillation. *Ind Eng Chem Res*. 2009;48:4474–4483.
15. Zavaleta R, Mccandless FP. Selective permeation through modified polyvinylidene fluoride membranes. *J Membr Sci*. 1976;1:333–353.
16. Mansourizadeh A, Ismail AF, Matsuura T. Effect of operating conditions on the physical and chemical CO2 absorption through the PVDF hollow fiber membrane contactor. *J Membr Sci*. 2010;353:192–200.
17. Grun M, Unger K, Matsumoto A, Tsutsumi K. Novel pathways for the preparations of mesoporous MCM-41 materials: control of porosity and morphology. *Microporous Mesoporous Mater*. 1999;27:207–216.
18. Hasegawa R, Takahash Y, Tadokoro H, Chatani Y. Crystal structures of three crystalline forms of poly (vinylidene fluoride). *Polym J*. 1972;3:600–610.
19. Lua AC, Su JC. Effects of carbonisation on pore evolution and gas permeation properties of carbon membranes from Kapton polyimide. *Carbon*. 2006;44:2964–2972.
20. Shen Y, Lua AC. Effects of membrane thickness and heat treatment on the gas transport properties of membranes based on P84 polyimide. *J Appl Poly Sci*. 2010;116:2906–2912.
21. Vu DQ, Koros WJ. Miller SJ. Mixed matrix membranes using carbon molecular sieves II. Modeling permeation behavior. *J Membr Sci*. 2003;211:335–348.
22. Matteucci S, Kusuma VA, Kelman SD, Freeman BD. Gas transport properties of MgO filled poly(1-trimethylsilyl-1-propyne) nanocomposites. *Polymer*. 2008;49:1659–1675.
23. Michaels AS, Parker RB. Sorption and flow gases in polyethylene. *J Poly Sci*. 1959;41:53–71.
24. Shen Y, Lua AC. Preparation and characterization of mixed matrix membranes based on PVDF and three inorganic fillers (fumed nonporous silica, zeolite 4A and mesoporous MCM-41) for gas separation. *Chem Eng J*. 2012; 192:201–210.
25. Higginsa S, McCoolb BA, Trippbc CP, Ruthvena DM, DeSistoab WJ. Covalent attachment of monochlorosilanes to mesoporous silica membranes using supercritical fluid deposition. *Sep Sci Technol*. 2008;43:4113–4128.
26. Ruthven D, Derrah R. Diffusion of monatomic and diatomic gases in 4A and 5A. *J Chem Soc Faraday Trans*. 1975;71:2031–2044.
27. Moore TT, Koros WJ. Gas sorption in polymers, molecular sieves, and mixed matrix membranes. *J Appl Poly Sci*. 2007;104:4053–4059.

Appendix A

The gas transport through MCM-41 particles is based on Knudsen diffusion and the corresponding permeability P_d is given by Eq. A1. The permeabilites of He, CO_2, O_2, and N_2 for the mesoporous MCM-41 particles were found to be 1.51×10^6, 3.2×10^5, 3.8×10^5, and 4.0×10^5 Barrer[25] at 298 K, respectively.

$$P_d = 97\left(\frac{r\varepsilon}{\tau}\right)\frac{1}{R\sqrt{TM}}\left(\text{mol}\times\text{m}^{-1}\times\text{s}^{-1}\times\text{Pa}^{-1}\right) \quad \text{(A1)}$$

where r is the mean pore diameter (m), ε is the porosity, τ is the tortuosity, R is the gas constant (J mol^{-1} K^{-1}), T is the absolute temperature, and M is the molecular weight. The r and ε/τ values were measured to be 2.7 nm and 0.59,[25] respectively.

The diffusion coefficients D_i of CO_2, O_2, and N_2 through zeolite 4A were calculated to be 8.7×10^{-10}, 3.2×10^{-9}, and 3.3×10^{-11} cm^2/s[26] at 298 K, respectively, using the Arrhenius formula.

$$D_i = D_0\exp\left(-E_d/RT\right) \quad \text{(A2)}$$

where the pre-exponential factor D_o and activated energy E_d were reported by Ruthven and Derrah.[26]

The solubility coefficients S_i of CO_2, O_2, and N_2 in zeolite 4A at 308 K were 2.97×10^{-1}, 1.78×10^{-3}, and 3.88×10^{-3} mol Pa^{-1} m^{-3},[27] respectively, according to Moore and Koros. The data were adjusted to 298 K using the Arrhenius formula,

Table A1. P_{eff}/P_c Modeling Results of P84/SiO_2 Composite Membranes Based on Maxwell Model, Higuchi Model, Bruggeman Model, and Bottcher-Landauer Model

	P_{eff}/P_c			
Volume Fraction	Maxwell	Higuchi	Bruggeman	Bottcher-Landauer
0	1	1	1	1
0.033	0.952	0.941	0.951	0.951
0.066	0.904	0.883	0.902	0.901
0.134	0.811	0.776	0.806	0.799
0.204	0.723	0.677	0.711	0.694
0.277	0.635	0.584	0.615	0.585

which were 5.38×10^{-1}, 2.12×10^{-3} and 4.91×10^{-3} mol Pa^{-1} m^{-3}, for CO_2, O_2 and N_2, respectively.[27]

$$S_i = S_0 \exp(-H_s/RT) \tag{A3}$$

where S_0 is the pre-exponential factor and H_s is the entropy change.

The permeability coefficients of CO_2, O_2, and N_2 in zeolite 4A are obtained as the product of the solubility coefficient and the diffusion coefficients at 298 K, which was 139.5, 2.0, and 0.048 Barrer, respectively.

Due to a lack of He diffusion and sorption data in zeolite 4A, the He permeability for zeolite 4A was estimated to be 1255.5 Barrer in accordance to the selectivity of He/CO_2 for the zeolite 4A membranes.

Appendix B
Sample Calculations for P84/SiO_2 Composite Membranes

Maxwell, Higuchi, Bruggeman, and Bottcher-Landauer model calculation results

The P84/SiO_2 MMMs with five different weight percentages (w_f) of SiO_2, that is, 4, 8, 16, 24, and 32%, were prepared. The weight percentage was converted into volume fraction (ϕ_d) using the following equation

$$\phi_d = \frac{w_f}{w_f + \frac{\rho_f}{\rho_p}(1-w_f)}$$

where ρ_f is the density of the inorganic nano-SiO_2 fillers, which was experimentally determined to be 2.17 g/cm^3, and ρ_p is the density of the PVDF polymer, which is related to the crystallinity (χ) of the PVDF by the following equation

$$\rho_p = \frac{1}{\frac{1-\chi}{\rho_{am}} + \frac{\chi}{\rho_{cr}}}$$

where ρ_{am} and ρ_{cr} are the densities of the amorphous and crystalline PVDF respectively, which were 1.68 and 1.92 g/cm^3, respectively. The crystallinity (χ) of the PVDF was calculated using the following equation

$$\chi = \frac{\Delta H}{W \times \Delta H^0} \times 100\%$$

where ΔH is the fusion heat of the membrane, W is the PVDF weight content in the composite membranes, ΔH^0 is the fusion heat of PVDF with 100% crystallinity of α phase, which was 90.4 J/mol.

Due to the fact that nano-silica is nonporous, the permeability of the dispersed phase (P_d) is 0 for P84/SiO_2 MMMs. Consequently, these four models could be simplified accordingly.

Maxwell model

$$P_{eff} = P_c \frac{2-2\phi_d}{2+\phi_d}$$

Higuchi model

$$P_{eff} = P_c \left[1 - \frac{6\phi_d}{3.22+2.78\phi_d}\right]$$

Bruggeman model

$$P_{eff} = P_c (1-\phi_d)^{3/2}$$

Bottcher-Landauer model

$$P_{eff} = P_c (2-3\phi_d)/2$$

The calculation results based on these models are shown in Table A1.

Modified Maxwell model without consideration for the crystalline effects on gas transport

First, Maxwell equation is used to obtain the permeability of the combined interface voids and inorganic phase with the interface void as the continuous phase and the inorganic phase as the dispersed phase.

$$P_{eff} = P_v \left[\frac{P_d + 2P_v - 2\phi(P_v - P_d)}{P_d + 2P_v + \phi(P_v - P_d)}\right]$$

where

$$P_v = \frac{9.7\times10^{-5} r}{RT}\sqrt{\frac{T}{M_A}}\left[1 - \frac{d_g}{2r}\right]^3$$

and

$$\phi = \frac{V_f}{V_f + V_v}$$

where, r is the effective pore radius, T is the temperature, M_A is the molecular weight, d_g is the gas molecular size, R is the gas constant, P_{eff} is the permeability of the combined dispersed or inorganic phase and interface void, P_d is the permeability of the dispersed or inorganic phase, P_v is the permeability of the interface voids, and V_f and V_v are the volumes of inorganic filler and voids, respectively.

Second, the value of the permeability of the combined filler and interface void, P_{eff}, can then be used along with the continuous polymer phase permeability, P_c, to obtain a predicted permeability P_{3MM} for the three-phase MMMs by applying Maxwell equation a second time.

$$P_{3MM} = P_c \left[\frac{P_{eff} + 2P_c - 2\phi'(P_c - P_{eff})}{P_{eff} + 2P_c + \phi'(P_c - P_{eff})}\right]$$

where

$$\phi' = \frac{V_f + V_v}{V_f + V_v + V_p}$$

and V_p is the polymer volume.

Because $P_{eff} >> P_c$, the permeability P_{3MMM} for the three-phase MMMs becomes

$$P_{3MM} = P_c \times \frac{1+2\phi'}{1-\phi'}$$

The void thickness was calculated using the following equation

Table B1. Modeling Permeability Results of P84/SiO_2 Composite Membranes Based on Maxwell Model without Consideration for the Crystalline Effects on Gas Transport

Nominal Volume Fraction	Void Thickness (angstrom)	P_v (Barrer)	P_{eff} (Barrer)	P_{3MM}/P_c
0.033	13.6	1289611	411700	1.51
0.066	13.9	1330536	432268	2.07
0.134	14.5	1412606	474638	3.34
0.204	15.2	1508690	526095	4.87
0.277	16.0	1618886	587482	6.78

$$l=\left[\left(\frac{a\left(1-\phi_f^N\right)+1}{1-a\phi_f^N}\right)^{1/3}-1\right]\times r$$

where a is the gradient of line for void volume fraction ϕ_V vs. inorganic filler nominal volume fraction and $\phi_f^N$is the inorganic nominal volume fraction.

The calculation results based on the modified Maxwell model without consideration for the crystalline effects on gas transport are shown in Table B1.

Extended modified Maxwell model with consideration for the crystalline and immobilization factor effects on gas transport

Considering the crystalline and immobilization factor effects on the transport properties of PVDF, the permeability P of PVDF can be calculated using the following equation

$$P=P^*\alpha^2/\beta$$

where $P^*$is the permeability of complete amorphous PVDF, which is 7.16, 2.15, 0.344, and 0.093 Barrer, for He, CO_2, O_2, and N_2 respectively. The immobilization factor, β, of crystalline polymer is dependent on the gas penetrant molecular size which is set to be 1.0, 1.2, 1.4, and 1.5 for He, CO_2, O_2, and N_2, respectively. The volume fraction of the amorphous polymer, α, can be determined by the crystallinity χ of the MMMs as follows

$$\alpha=1-\chi$$

The introduction of silica into PVDF matrix will introduce the voids as well as variations in PVDF crystallinity. Both these two factors will affect the gas transport properties of the resulting composite membranes. Applying the extended modified Maxwell model and considering the crystalline and immobilization factor effects on the gas transport properties of PVDF, the permeability of the resulting composite membranes can be obtained and the results are shown in Table B2.

Table B2. Modeling and Experimental Permeability Results of P84/SiO_2 Composite Membranes with Consideration for the Crystalline and Immobilization Factor Effects on Gas Transport

Nominal Volume Fraction	Modeling Results (Barrer)				Experimental Results (Barrer)			
	He	CO_2	O_2	N_2	He	CO_2	O_2	N_2
0	3.83	1.09	0.14	0.036	3.94	1.18	0.14	0.041
0.033	3.40	0.97	0.12	0.032	3.62	0.92	0.12	0.033
0.066	3.78	1.08	0.14	0.035	4.19	1.15	0.17	0.043
0.134	5.09	1.45	0.18	0.048	5.42	1.64	0.23	0.06
0.204	7.12	2.03	0.26	0.067	8.01	2.45	0.32	0.072
0.277	8.71	2.47	0.31	0.082	8.87	2.65	0.36	0.084

Manuscript received Mar. 4, 2013, and revision received Jun. 3, 2013.